Hindawi Publishing Corporation
Smart Materials Research
Volume 2013, Article ID 767019, 8 pages
http://dx.doi.org/10.1155/2013/767019

Research Article

Reflection and Transmission Phenomena in Poroelastic Plate Sandwiched between Fluid Half Space and Porous Piezoelectric Half Space

Vishakha Gupta[1] and Anil K. Vashishth[2]

[1] *Department of Mathematics, Dyal Singh College, Karnal 132 001, India*
[2] *Department of Mathematics, Kurukshetra University, Kurukshetra 136 119, India*

Correspondence should be addressed to Vishakha Gupta; vi_shu85@yahoo.co.in

Received 25 April 2013; Accepted 22 June 2013

Academic Editor: Chris Bowen

The reflection and transmission of elastic waves in porous piezoelectric plate, overlying a porous piezoelectric half space and underlying a fluid half space, is studied. The constitutive and governing equations are formulated for porous piezoelectric materials. The expressions for the mechanical displacements, electric displacements, stresses, and electric potentials are derived for porous piezoelectric plate, porous piezoelectric half space, and fluid half space. The boundary conditions are described for the studied model. The behaviour of reflected and transmitted amplitude ratios relative to frequency, incident angle, thickness, and porosity is observed numerically. The impedance mismatching problem between the dense piezoelectric materials and the surrounding medium can be solved by the inclusion of porosity in dense piezoceramics.

1. Introduction

The field of smart materials (piezoelectric) has advanced rapidly due to an increasing awareness about capabilities of such materials, the development of new materials and transducer designs, and increasingly stringent design and control specifications in aerospace, aeronautics, industrial, automotive, biomedical, and nanosystems. Piezoelectric materials are brittle in nature which leads to the failure of devices. It is commonly found that 5% porosity exists in piezoelectric materials which are considered as manufacturing defects. Instead of considering it as a manufacturing defect, such materials can be modelled as porous piezoelectric materials. Porous piezoelectric materials are widely used in ultrasonic transducers, hydrophones, and pressure sensors. Porous ceramics are of interest for ultrasonic transducer applications. Porosity allows to decrease the acoustic impedance, thus improving transfer of acoustic energy to water or biological tissues. For underwater applications, the figure of merit can also be improved as compared to dense material. The surface impedance of porous piezoelectric materials is less as compared to dense piezoelectric materials. Alvarez-Arenas and De Espinosa [1] made a study related to characterization of porous piezoelectric ceramic. The experimental study on wave propagation in composite structures was done by Alvarez-Arenas et al. [2]. Different authors [3, 4] developed models related to synthesis, fabrication, and processing of porous piezoelectric materials. Kumar et al. [5] investigated the effects of porosity and pore forming agents in porous piezoceramics.

The influence of piezoelectricity on the reflection-transmission phenomena in fluid-loaded piezoelectric half space and fluid-loaded piezoelectric plate was studied by Nayfeh and Chien [6, 7]. Darinskii and Weihnacht [8] studied theoretically the propagation and the generation of leaky waves in a fluid layer enclosed between the half-infinite lithium niobate substrate coated with a thin silicon oxide layer and the half-infinite domain occupied by silicon rubber. Love waves propagating in a layered structure with an elastic layer deposited on a piezoelectric substrate were analytically investigated by Liu and He [9]. Vashishth and Gupta [10] derived the constitutive equations for porous piezoelectric materials. The characteristics of waves propagating in porous piezoelectric materials were studied analytically

and numerically by Vashishth and Gupta [11]. The general theorems of elasticity were extended for the linear theory of elasticity for porous piezoelectric materials by Vashishth and Gupta [12]. The reflection and transmission of waves from fluid-loaded porous piezoelectric half space was studied by Vashishth and Gupta [13].

The fabrication of piezoelectric transducers for high resolution medical imagining applications requires a backing material to damp the piezoelectric resonance, resulting in a short time resonance, that is, improved resolution. Thus, the choice of such a substrate must be made according to its acoustical properties. For ultrasonic transducer model, a thick film of porous piezoelectric material has to be deposited on a porous piezoelectric substrate. Levassort et al. [14] and Marechal et al. [15] developed experimental models to study the properties of integrated structures for ultrasonic imaging application purpose. These integrated structures contain a porous piezoelectric layer overlying a porous piezoelectric substrate.

Motivated the theoretical and experimental models developed to study the properties of the integrated structures for ultrasonic imaging applications and transducer application, a theoretical model is developed in this paper to study the effects of porosity, thickness, and incidence angle on the reflection-transmission phenomena. In the present paper, the effects of piezoelectricity, frequency, porosity, incidence angle, and thickness on the amplitude ratios corresponding to reflected and transmitted waves in fluid-loaded porous piezoelectric plate are studied analytically as well as numerically for a particular model. The results obtained in this paper can be used to improve the properties of porous piezoelectric materials.

2. Formulation of the Problem

Let us consider a porous piezoelectric plate of thickness h overlying a porous piezoelectric half space and underlying a fluid half space. An elastic wave from the fluid half space making an angle θ with x_3 axis is assumed to strike the interface $x_3 = 0$ which results into one reflected wave in fluid half space and five transmitted waves in porous piezoelectric half space.

The constitutive equations for transversely isotropic porous piezoelectric material are

$$\begin{bmatrix} \sigma_1 \\ \sigma_2 \\ \sigma_3 \\ \sigma_4 \\ \sigma_5 \\ \sigma_6 \\ \sigma^* \\ D_1 \\ D_2 \\ D_3 \\ D_1^* \\ D_2^* \\ D_3^* \end{bmatrix} = \begin{bmatrix} c_{11} & c_{12} & c_{13} & 0 & 0 & 0 & m_{11} & 0 & 0 & -e_{31} & 0 & 0 & -\zeta_{31} \\ c_{12} & c_{11} & c_{13} & 0 & 0 & 0 & m_{11} & 0 & 0 & -e_{31} & 0 & 0 & -\zeta_{31} \\ c_{13} & c_{13} & c_{33} & 0 & 0 & 0 & m_{33} & 0 & 0 & -e_{33} & 0 & 0 & -\zeta_{33} \\ 0 & 0 & 0 & c_{44} & 0 & 0 & 0 & 0 & -e_{15} & 0 & 0 & -\zeta_{15} & 0 \\ 0 & 0 & 0 & 0 & c_{44} & 0 & 0 & -e_{15} & 0 & 0 & -\zeta_{15} & 0 & 0 \\ 0 & 0 & 0 & 0 & 0 & \frac{(c_{11}-c_{12})}{2} & 0 & 0 & 0 & 0 & 0 & 0 & 0 \\ m_{11} & m_{11} & m_{33} & 0 & 0 & 0 & R & 0 & 0 & -\tilde{\zeta}_3 & 0 & 0 & -e_3^* \\ 0 & 0 & 0 & 0 & e_{15} & 0 & 0 & \xi_{11} & 0 & 0 & A_{11} & 0 & 0 \\ 0 & 0 & 0 & e_{15} & 0 & 0 & 0 & 0 & \xi_{11} & 0 & 0 & A_{11} & 0 \\ e_{31} & e_{31} & e_{33} & 0 & 0 & 0 & \tilde{\zeta}_3 & 0 & 0 & \xi_{33} & 0 & 0 & A_{33} \\ 0 & 0 & 0 & 0 & \zeta_{15} & 0 & 0 & A_{11} & 0 & 0 & \xi_{11}^* & 0 & 0 \\ 0 & 0 & 0 & \zeta_{15} & 0 & 0 & 0 & 0 & A_{11} & 0 & 0 & \xi_{11}^* & 0 \\ \zeta_{31} & \zeta_{31} & \zeta_{33} & 0 & 0 & 0 & e_3^* & 0 & 0 & A_{33} & 0 & 0 & \xi_{33}^* \end{bmatrix} \begin{bmatrix} \varepsilon_1 \\ \varepsilon_2 \\ \varepsilon_3 \\ 2\varepsilon_4 \\ 2\varepsilon_5 \\ 2\varepsilon_6 \\ \varepsilon^* \\ E_1 \\ E_2 \\ E_3 \\ E_1^* \\ E_2^* \\ E_3^* \end{bmatrix}. \quad (1)$$

Here, c_{ij} are the elastic stiffness tensor components of porous bulk material. R is elastic constant corresponding to fluid phase. e_{31}, e_{33}, e_{15}, ζ_{31}, ζ_{33}, ζ_{15}, e_3^*, and $\tilde{\zeta}_3$ are piezoelectric coefficients. ξ_{11}, ξ_{33}, A_{11}, A_{33}, ξ_{11}^*, and ξ_{33}^* are the dielectric coefficients. m_{11} and m_{33} are elastic coupling coefficients. σ_{ij}, D_i, and E_i are the stress tensor components, electric displacements, and electric field vector for the solid phases of the porous aggregate, respectively. The corresponding quantities with superscript * are associated with the fluid phase.

The equations of motion are

$$\begin{aligned} \sigma_{ij,j} &= \rho_{11}\ddot{u}_j + \rho_{12}\ddot{U}_j, \\ \sigma_{,i}^* &= \rho_{12}\ddot{u}_j + \rho_{22}\ddot{U}_j, \\ D_{i,i} &= 0, \\ D_{i,i}^* &= 0, \end{aligned} \quad (2)$$

ρ_{11}, ρ_{12}, and ρ_{22} are the dynamical coefficients.

For a harmonic plane wave, the associated physical quantities can be represented as

$$\begin{aligned} &(u_i, U_i, \psi, \psi^*) \\ &\quad = (A_i, B_i, G, H) \exp\left(\iota\omega\left(\frac{1}{c}x_1 + px_3 - t\right)\right), \quad (i = 1, 3), \end{aligned} \quad (3)$$

where p is, unknown parameter and $(A_1, A_3, B_1, B_3, G, H)$ are the amplitudes associated with the harmonic wave. c is the apparent phase velocity. ψ and ψ^* are the electric potentials corresponding to solid and fluid phases.

Equations (1)–(3) imply

$$c_1 p^{10} + c_2 p^8 + c_3 p^6 + c_4 p^4 + c_5 p^2 + c_6 = 0, \quad (4)$$

$c_{11} = 148.0e9$, $c_{12} = 76.2e9$, $c_{13} = 74.2e9$, $c_{33} = 131.0e9$, $c_{44} = 25.3e9$, $m_{11} = 8.8e9$, $m_{33} = 5.2e9$, $R = 20e9$, $e_{15} = 9.3$, $e_{31} = -2.324$, $e_{33} = 10.99$, $\zeta_{15} = 2.72$, $\zeta_{31} = -0.48$, $\zeta_{33} = 5.32$, $e_3^* = -3.6$, $\tilde{\zeta}_3 = -7.5$, $\xi_{11} = 3.984e-9$, $\xi_{33} = 2.081e-9$, $\xi_{11}^* = 11.8e-9$, $\xi_{33}^* = 13.9e-9$, $A_{11} = 12.8e-9$, $A_{33} = 15.1e-9$, $f = 0.2$, c_f (m/s) = 1500, ρ (kg/m^3) = 7700, $\rho_{11} = 0.66 \times 7700$, $\rho_{12} = -0.15 \times 7700$, $\rho_{22} = 0.66 \times 7700$.

Box 1: Elastic constants, piezoelectric constants, and dielectric constants of PZT crystal.

where coefficients c_i $(i = 1, 2, \ldots, 6)$ are listed in the appendix. p_i $(i = 1, 2, \ldots, 5)$ corresponds to the roots whose real part are positive while p_i $(i = 6, \ldots, 10)$ corresponds to the roots whose real parts are negative. p_1, p_2, and p_3 correspond to slowness of quasi-P_1 mode, quasi-S_1 mode, and quasi-P_2 mode, and p_4 and p_5 correspond to electric potential modes. These roots of (4) are arranged such that

$$p_{i+5} = -p_i, \quad (i = 1, 2, \ldots, 5). \tag{5}$$

Thus, we can write

$$\begin{aligned}&(u_1, u_3, U_1, U_3, \psi, \psi^*)\\ &= \sum_{i=1}^{10} (1, u_{1i}, u_{2i}, u_{3i}, u_{4i}, u_{5i}) A_{1i} \exp\left(\iota\omega\left(\frac{1}{c}x_1 + p_i x_3 - t\right)\right).\end{aligned} \tag{6}$$

Using (1) and (6), we obtain

$$\begin{aligned}&(\sigma_{31}, \sigma_{33}, \sigma^*, D_3, D_3^*)\\ &= \sum_{i=1}^{10} (d_{1i}, d_{2i}, d_{3i}, d_{4i}, d_{5i}) A_{1i} \exp\left(\iota\omega\left(\frac{1}{c}x_1 + p_i x_3 - t\right)\right),\end{aligned} \tag{7}$$

where d_{ki}, $(k = 1, 2, \ldots, 5)$ are given in the appendix.

Similarly, the corresponding expressions in the porous piezoelectric half space are

$$\begin{aligned}&\left(u_1^{hf}, u_3^{hf}, U_1^{hf}, U_3^{hf}, \psi^{hf}, \psi^{*hf}\right)\\ &= \sum_{i=1}^{5} \left(1, u_{1i}^{hf}, u_{2i}^{hf}, u_{3i}^{hf}, u_{4i}^{hf}, u_{5i}^{hf}\right) B_{1i}\\ &\quad \times \exp\left(\iota\omega\left(\frac{1}{c}x_1 + p_i^{hf} x_3 - t\right)\right),\\ &\left(\sigma_{31}^{hf}, \sigma_{33}^{hf}, \sigma^{*hf}, D_3^{hf}, D_3^{*hf}\right)\\ &= \sum_{i=1}^{5} \left(d_{1i}^{hf}, d_{2i}^{hf}, d_{3i}^{hf}, d_{4i}^{hf}, d_{5i}^{hf}\right) B_{1i}\\ &\quad \times \exp\left(\iota\omega\left(\frac{1}{c}x_1 + p_i^{hf} x_3 - t\right)\right).\end{aligned} \tag{8}$$

The normal displacement and normal stress in the fluid half space can be written as

$$\begin{aligned}u_3^f &= \rho^f c \left[U_1^f \exp\left(\iota\omega\left(\frac{1}{c}x_1 + p_f x_3 - t\right)\right)\right.\\ &\quad \left. - U_2^f \exp\left(\iota\omega\left(\frac{1}{c}x_1 - p_f x_3 - t\right)\right)\right],\\ \sigma_{33}^f &= \iota\omega\rho^f c \left[U_1^f \exp\left(\iota\omega\left(\frac{1}{c}x_1 + p_f x_3 - t\right)\right)\right.\\ &\quad \left. - U_2^f \exp\left(\iota\omega\left(\frac{1}{c}x_1 - p_f x_3 - t\right)\right)\right],\end{aligned} \tag{9}$$

where $p^f = (1/c)\sqrt{c^2/(c^f)^2 - 1}$.

Here, c_f and ρ^f are the longitudinal incident wave velocity and density in the fluid medium.

The boundary conditions at the interface $x_3 = 0$ are

$$\begin{aligned}&\sigma_{33} = (1 - f)\sigma_{33}^f, \qquad \sigma^* = f\sigma_{33}^f,\\ &(1 - f)\dot{u}_3 + f\dot{U}_3 = \dot{u}_3^f, \qquad D_3 = 0,\\ &D_3^* = 0, \qquad \sigma_{13} = 0.\end{aligned} \tag{10}$$

The boundary conditions at the interface $x_3 = h$ are

$$\begin{aligned}&u_1 = u_1^{hf}, \qquad u_3 = u_3^{hf}, \qquad U_3 = U_3^{hf},\\ &\psi = \psi^{hf}, \qquad \psi^* = \psi^{*hf}, \qquad \sigma_{33} = \sigma_{33}^{hf},\\ &\sigma^{*hf} = \sigma_{33}^{hf}, \qquad \sigma_{13} = \sigma_{13}^{hf}, \qquad D_3 = D_3^{hf},\\ &D_3^* = D_3^{*hf}.\end{aligned} \tag{11}$$

$c_{11} = 148.0e9$, $c_{12} = 76.2e9$, $c_{13} = 74.2e9$, $c_{33} = 131.0e9$, $c_{44} = 25.3e9$, $m_{11} = 8.8e9$, $m_{33} = 5.2e9$, $R = 20e9$, $e_{15} = 9.3$, $e_{31} = -2.324$, $e_{33} = 10.99$, $\zeta_{15} = 2.72$, $\zeta_{31} = -0.48$, $\zeta_{33} = 5.32$, $e_3^* = -3.6$, $\tilde{\zeta}_3 = -7.5$, $\xi_{11} = 3.984e-9$, $\xi_{33} = 2.081e-9$, $\xi_{11}^* = 11.8e-9$, $\xi_{33}^* = 13.9e-9$, $A_{11} = 12.8e-9$, $A_{33} = 15.1e-9$, $\rho\ (\mathrm{kg/m^3}) = 5700$.

Box 2: Elastic constants, piezoelectric constants, and dielectric constants of $BaTiO_3$ crystal.

Making use of (6)–(9) into (10) and (11), we obtain the following nonhomogeneous system:

$$AX = B, \tag{12}$$

where

$$A = \begin{bmatrix} e_1 & \cdots & e_{10} & e_1^{hf} & \cdots & \cdots & \cdots & e_5^{hf} & 0 \\ u_{11}e_1 & \cdots & u_{1,10}e_{10} & u_{11}^{hf}e_1^{hf} & \cdots & \cdots & \cdots & u_{15}^{hf}e_5^{hf} & 00 \\ u_{31}e_1 & \cdots & u_{1,10}e_{10} & u_{31}^{hf}e_1^{hf} & \cdots & \cdots & \cdots & u_{35}^{hf}e_5^{hf} & 00 \\ u_{41}e_1 & \cdots & u_{4,10}e_{10} & u_{41}^{hf}e_1^{hf} & \cdots & \cdots & \cdots & u_{45}^{hf}e_5^{hf} & 00 \\ u_{51}e_1 & \cdots & u_{5,10}e_{10} & u_{51}^{hf}e_1^{hf} & \cdots & \cdots & \cdots & u_{55}^{hf}e_5^{hf} & 00 \\ d_{11}e_1 & \cdots & d_{1,10}e_{10} & d_{11}^{hf}e_1^{hf} & \cdots & \cdots & \cdots & d_{15}^{hf}e_5^{hf} & 00 \\ d_{21}e_1 & \cdots & d_{2,10}e_{10} & d_{21}^{hf}e_1^{hf} & \cdots & \cdots & \cdots & d_{25}^{hf}e_5^{hf} & 00 \\ d_{31}e_1 & \cdots & d_{3,10}e_{10} & d_{31}^{hf}e_1^{hf} & \cdots & \cdots & \cdots & d_{35}^{hf}e_5^{hf} & 00 \\ d_{41}e_1 & \cdots & d_{4,10}e_{10} & d_{41}^{hf}e_1^{hf} & \cdots & \cdots & \cdots & d_{45}^{hf}e_5^{hf} & 00 \\ d_{51}e_1 & \cdots & d_{5,10}e_{10} & d_{51}^{hf}e_1^{hf} & \cdots & \cdots & \cdots & d_{55}^{hf}e_5^{hf} & 00 \\ d_{21} & \cdots & d_{2,10} & 0 & 0 & 0 & 0 & 0 & \iota(1-f)\omega\rho^f c \\ d_{31} & \cdots & d_{3,10} & 0 & 0 & 0 & 0 & 0 & \iota f\omega\rho^f c \\ (1-f)u_{11} + fu_{31} & \cdots & (1-f)u_{1,10} + fu_{3,10} & 0 & 0 & 0 & 0 & 0 & \rho^f c \\ d_{41} & \cdots & d_{4,10} & 0 & 0 & 0 & 0 & 0 & 0 \\ d_{51} & \cdots & d_{5,10} & 0 & 0 & 0 & 0 & 0 & 0 \\ d_{11} & \cdots & d_{1,10} & 0 & 0 & 0 & 0 & 0 & 0 \end{bmatrix}, \tag{13}$$

$$B = \left[0\ \ 0\ \ 0\ \ 0\ \ 0\ \ 0\ \ 0\ \ 0\ \ 0\ \ 0\ \ \iota(1-f)\omega\rho^f c\ \ \iota f\omega\rho^f c\ \ \rho^f c\ \ 0\ \ 0\ \ 0\right]^T,$$

$$X = \left[A_{11}\ \ A_{12}\ \ \cdots\ \ A_{1,10}\ \ B_{11}\ \ \cdots\ \ B_{15}\ \ R'\right]^T,$$

$$e_i = \exp\left(\iota\omega p_i h\right), \quad (i = 1, 2, \ldots, 10),$$

$$e_i^{hf} = \exp\left(\iota\omega p_i^{hf} h\right), \quad (i = 1, \ldots, 5).$$

On solving nonhomogeneous system (12), the reflected and transmitted amplitude ratios can be obtained.

3. Numerical Study

The reflected and transmitted amplitude ratios are calculated numerically for a particular model. The material of the porous piezoelectric plate is taken as PZT and that of porous piezoelectric half space is taken as $BaTiO_3$. A_R represents the reflected amplitude ratio. A_1, A_2, and A_3 represent transmitted amplitude ratios corresponding to quasi-P_1, quasi-S_1 and quasi-P_2 waves. The frequency, thickness of layer, incidence angle and porosity are assumed 1 MHz, 0.001, 5°, and 0.2, respectively unless specified otherwise. Following Gupta and Venkatesh [16], the elastic, piezoelectric, dielectric coefficients and other parameters used in the study for these ceramics are given in Boxes 1 and 2.

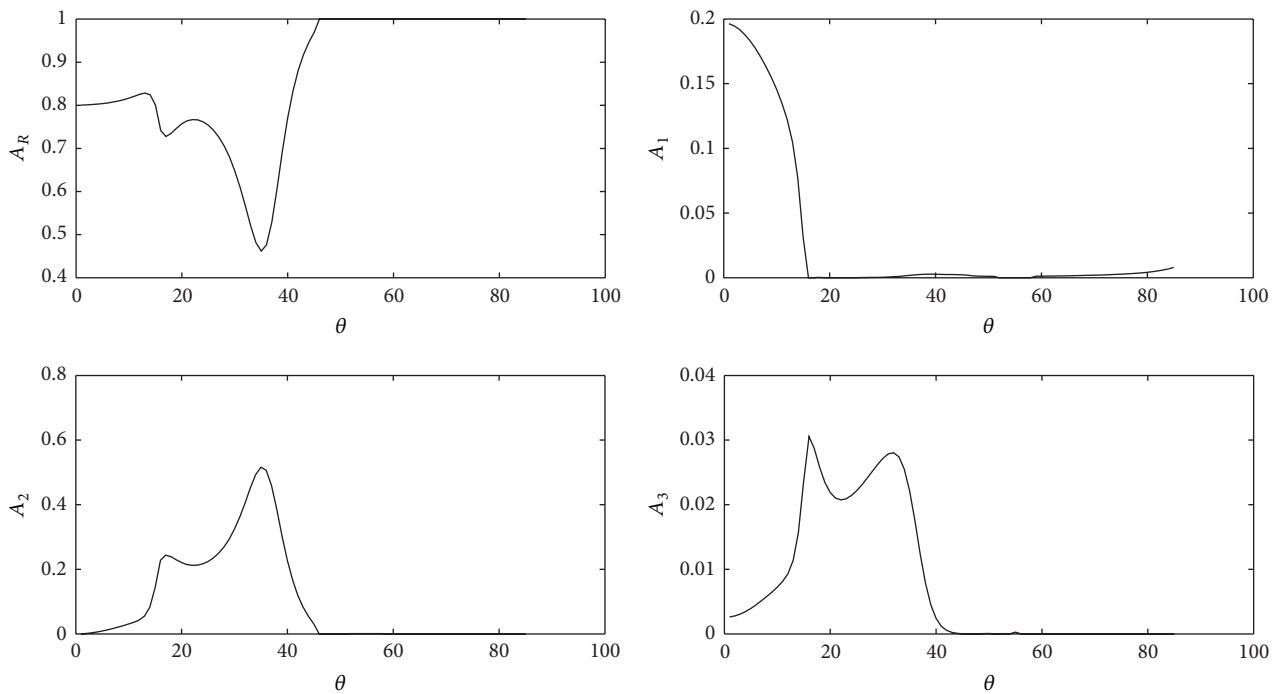

Figure 1: Behaviour of reflected and transmitted amplitude ratios with angle of incidence at fixed frequency.

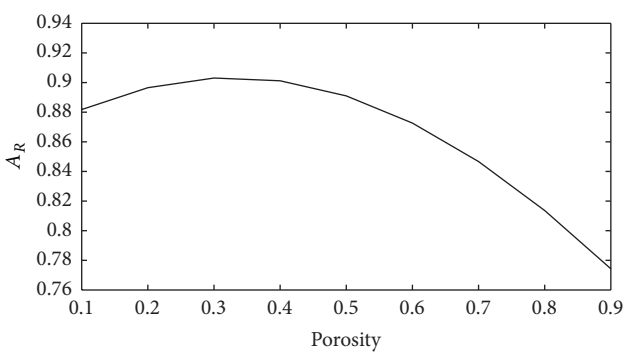

Figure 2: Behaviour of reflected amplitude ratio with porosity at fixed angle of incidence and fixed frequency.

Figure 1 shows the behaviour of amplitude ratios relative to incidence angle. The reflected amplitude ratio becomes unity after critical angle $\theta = 42^\circ$. After this critical angle, all the transmitted modes become nonpropagating. Before $\theta = 13^\circ$, all the transmitted modes propagate in the medium. Less amount of incident energy gets transmitted into the medium.

Figure 2 depicts the effects of porosity on the reflected amplitude ratio. It is observed that the reflected amplitude ration decreases with increase in porosity. Thus, as the porosity of the piezoelectric materials increases, more amount of incident energy gets transmitted into the medium.

The behaviour of amplitude ratios with frequency in the frequency range 1 MHz–11 MHz is observed in Figure 3. The behaviour of reflected amplitude ratio with frequency is oscillatory and repeats itself in small frequency pockets. The pattern of variation of reflected amplitude ratio is symmetric while that of transmitted amplitude ratios is not symmetric. The frequencies at which reflected amplitude ratio is maximum or minimum give important information in the design of transducers.

The effect of thickness of the porous piezoelectric plate sandwiched between fluid half space and porous piezoelectric half space on the behaviour of amplitude ratios relative to frequency is observed in Figure 4. The thickness of the plate is assumed 1 mm, 2 mm, 3 mm, and 4 mm in respective figures. It is observed that change in the thickness of the plate does not affect the behaviour corresponding to quasi-P_1 wave. The number of maxima/minima increases with increase in the thickness of the plate. Thus, with increase in the thickness of the plate we can find more frequencies at which reflection is very low or very high.

4. Conclusion

The reflection and transmission phenomenon in porous piezoelectric plate sandwiched between fluid half space and porous piezoelectric half space is studied. The behaviour of reflected and transmitted amplitude ratios relative to frequency, angle of incidence, layer thickness, and porosity is observed numerically for a particular model. The amplitude ratios are found to be sensitive with respect to frequency and incidence angle. The number of maxima/minima increases with increase in the thickness of the layer. With increase in porosity of the medium, less amount of incident energy gets reflected back.

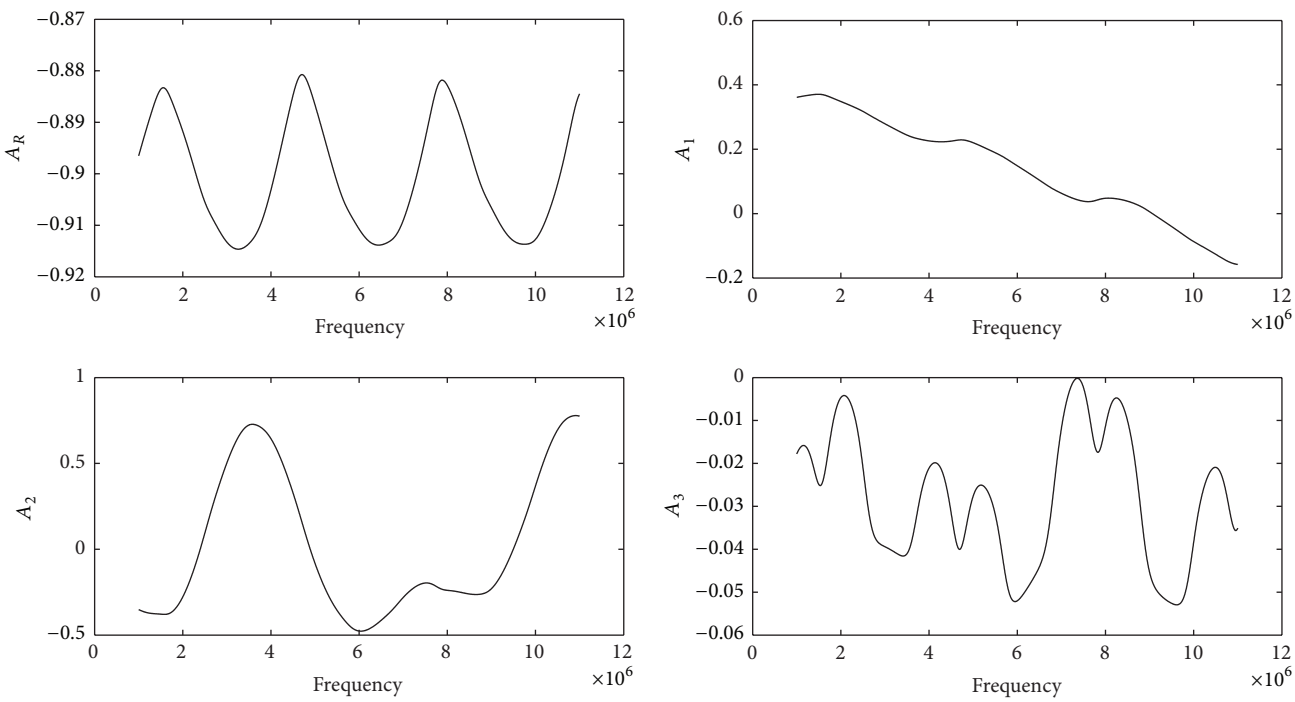

Figure 3: Behaviour of reflected and transmitted amplitude ratios with frequency at fixed angle of incidence.

Appendix

We have the following:

$$c_1 = \beta_1 y_1 - \beta_5 y_{10} + \beta_9 y_{17} - \beta_{13} y_{26},$$

$$c_2 = \beta_2 y_1 + \beta_1 y_2 - \beta_6 y_{10} - \beta_5 y_{11} + \beta_{10} y_{17} + \beta_9 y_{18} - \beta_{14} y_{26} - \beta_{13} y_{27},$$

$$c_3 = \beta_3 y_1 + \beta_2 y_2 + \beta_1 y_3 - \beta_7 y_{10} - \beta_6 y_{11} + \beta_{11} y_{17} + \beta_{10} y_{18} + \beta_9 y_{19} - \beta_{15} y_{26} - \beta_{14} y_{27} - \beta_{13} y_{28},$$

$$c_4 = \beta_4 y_1 + \beta_3 y_2 + \beta_2 y_3 - \beta_8 y_{10} - \beta_7 y_{11} + \beta_{12} y_{17} + \beta_{11} y_{18} + \beta_{10} y_{19} - \beta_{16} y_{26} - \beta_{15} y_{27} - \beta_{14} y_{28},$$

$$c_5 = \beta_4 y_2 + \beta_3 y_3 + \beta_{12} y_{18} + \beta_{11} y_{19} - \beta_8 y_{11} - \beta_{16} y_{27} - \beta_{15} y_{28},$$

$$c_6 = \beta_4 y_3 + \beta_{12} y_{19} - \beta_{16} y_{28},$$

$$\beta_1 = q_1 y_{12} - q_4 y_{14} + q_7 y_{15},$$

$$\beta_2 = q_2 y_{12} + q_1 y_{13} - q_5 y_{14} + q_8 y_{15} + q_7 y_{16},$$

$$\beta_3 = q_3 y_{12} + q_2 y_{13} - q_6 y_{14} + q_9 y_{15} + q_8 y_{16},$$

$$\beta_4 = q_3 y_{13} + q_9 y_{16}, \qquad \beta_5 = q_1 y_4 - q_4 y_6 + q_7 y_8,$$

$$\beta_6 = q_2 y_4 + q_1 y_5 - q_5 y_6 - q_4 y_7 + q_8 y_8 + q_7 y_9,$$

$$\beta_7 = q_3 y_4 + q_2 y_5 - q_6 y_6 - q_5 y_7 + q_9 y_8 + q_8 y_9,$$

$$\beta_8 = q_3 y_5 - q_6 y_7 + q_9 y_9, \qquad \beta_9 = r_1 y_4 - r_4 y_6 + r_7 y_8,$$

$$\beta_{10} = r_2 y_4 + r_1 y_5 - r_5 y_6 - r_4 y_7 + r_8 y_8 + r_7 y_9,$$

$$\beta_{11} = r_3 y_4 + r_2 y_5 - r_6 y_6 - r_5 y_7 + r_9 y_8 + r_8 y_9,$$

$$\beta_{12} = r_3 y_5 - r_6 y_7 + r_9 y_9, \qquad \beta_{13} = s_1 y_4 - s_4 y_6 + s_7 y_8,$$

$$\beta_{14} = s_2 y_4 + s_1 y_5 - s_5 y_6 - s_4 y_7 + s_8 y_8 + s_7 y_9,$$

$$\beta_{15} = s_3 y_4 + s_2 y_5 - s_6 y_6 - s_5 y_7 + s_9 y_8 + s_8 y_9,$$

$$\beta_{16} = s_3 y_5 - s_6 y_7 + s_9 y_9,$$

$$q_1 = y_{22} y_{33} - y_{24} y_{31},$$

$$q_2 = y_{22} y_{34} + y_{23} y_{33} - y_{25} y_{31} - y_{24} y_{32},$$

$$q_3 = y_{23} y_{34} - y_{25} y_{32}, \qquad q_4 = y_{20} y_{33} - y_{24} y_{29},$$

$$q_5 = y_{20} y_{34} + y_{21} y_{33} - y_{24} y_{30} - y_{25} y_{29},$$

$$q_6 = y_{21} y_{34} - y_{25} y_{30}, \qquad q_7 = y_{20} y_{31} - y_{22} y_{29},$$

$$q_8 = y_{20} y_{32} + y_{21} y_{31} - y_{23} y_{29} - y_{22} y_{30},$$

$$q_9 = y_{21} y_{32} - y_{23} y_{30},$$

$$r_1 = y_{14} y_{33} - y_{15} y_{31}, \qquad r_2 = y_{14} y_{34} - y_{16} y_{31} - y_{15} y_{32},$$

$$r_3 = -y_{16} y_{32}, \qquad r_4 = y_{12} y_{33} - y_{15} y_{29},$$

$$r_5 = y_{12} y_{34} + y_{13} y_{33} - y_{16} y_{29} - y_{15} y_{30},$$

$$r_6 = y_{13} y_{34} - y_{16} y_{30}, \qquad r_7 = y_{12} y_{31} - y_{14} y_{29},$$

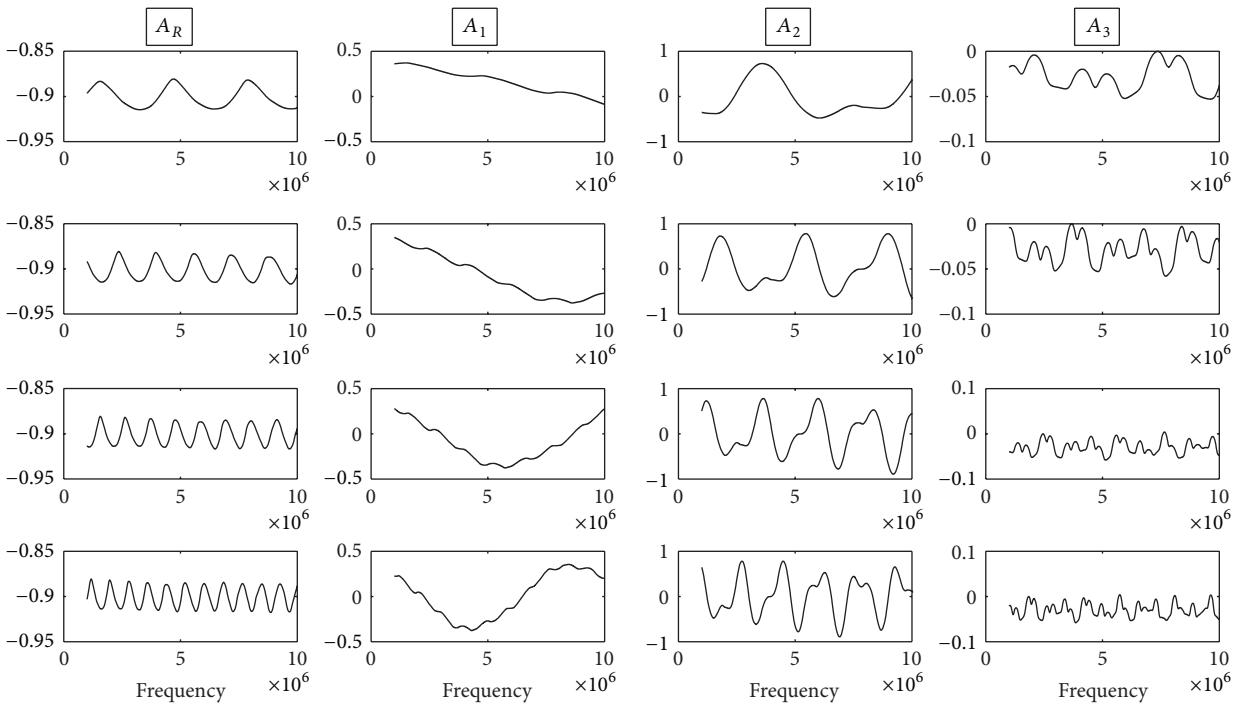

Figure 4: Effects of thickness of plate on the behaviour of amplitude ratios with frequency.

$$r_8 = y_{12}y_{32} - y_{14}y_{30} + y_{13}y_{31}, \qquad r_9 = y_{13}y_{32},$$

$$s_1 = y_{14}y_{24} - y_{15}y_{22}, \qquad s_2 = y_{14}y_{25} - y_{16}y_{22} - y_{15}y_{23},$$

$$s_3 = -y_{16}y_{23}, \qquad s_4 = y_{12}y_{24} - y_{15}y_{20},$$

$$s_5 = y_{12}y_{25} + y_{13}y_{24} - y_{16}y_{20} - y_{15}y_{21},$$

$$s_6 = y_{13}y_{25} - y_{16}y_{21}, \qquad s_7 = y_{12}y_{22} - y_{14}y_{20},$$

$$s_8 = y_{12}y_{23} - y_{14}y_{21} + y_{13}y_{22}, \qquad s_9 = y_{13}y_{23},$$

$$y_1 = e_{33}x_1 + \zeta_{33}x_6,$$

$$y_2 = \frac{(e_{15}x_1 + \zeta_{15}x_6)}{c^2} + \frac{(c_{44} + c_{13})}{c} + e_{33}x_2 + \zeta_{33}x_7,$$

$$y_3 = \frac{(e_{15}x_2 + \zeta_{15}x_7)}{c^2}, \qquad y_4 = e_{33}x_3 + \zeta_{33}x_8 + c_{33},$$

$$y_5 = \frac{(e_{15}x_3 + \zeta_{15}x_8 + c_{44})}{c^2} - \overline{\rho}_{33}^{11}, \qquad y_6 = e_{33}x_4 + \zeta_{33}x_9 + \frac{m_{33}}{c},$$

$$y_7 = \frac{(e_{15}x_4 + \zeta_{15}x_9)}{c^2}, \qquad y_8 = e_{33}x_5 + \zeta_{33}x_{10} + m_{33},$$

$$y_9 = \frac{(e_{15}x_5 + \zeta_{15}x_{10})}{c^2} - \overline{\rho}_{33}^{12}, \qquad y_{10} = \widetilde{\zeta}_3 x_1 + e_3^* x_6,$$

$$y_{11} = \frac{m_{11}}{c} + \widetilde{\zeta}_3 x_2 + e_3^* x_7, \qquad y_{12} = m_{33} + \widetilde{\zeta}_3 x_3 + e_3^* x_8,$$

$$y_{13} = -\overline{\rho}_{33}^{12}, \qquad y_{14} = \frac{R}{c} + \widetilde{\zeta}_3 x_4 + e_3^* x_9,$$

$$y_{15} = R + \widetilde{\zeta}_3 x_5 + e_3^* x_{10}, \qquad y_{16} = -\overline{\rho}_{33}^{22},$$

$$y_{17} = -x_1\xi_{33} - x_6 A_{33},$$

$$y_{18} = \frac{(-x_1\xi_{11} - x_6 A_{11})}{c^2} + \frac{(e_{15} + e_{31})}{c} - \xi_{33}x_2 - A_{33}x_7,$$

$$y_{19} = -\frac{(x_2\xi_{11} + x_7 A_{11})}{c^2}, \qquad y_{20} = e_{33} - x_3\xi_{33} - x_8 A_{33},$$

$$y_{21} = \frac{(e_{15} - x_3\xi_{11} - x_8 A_{11})}{c^2}, \qquad y_{22} = \frac{\widetilde{\zeta}_3}{c} - A_{33}x_9 - \xi_{33}x_4,$$

$$y_{23} = -\frac{(x_4\xi_{11} + x_9 A_{11})}{c^2}, \qquad y_{24} = -x_{10}A_{33} - x_5\xi_{33} + \widetilde{\zeta}_3,$$

$$y_{25} = -\frac{(x_5\xi_{11} + x_{10}A_{11})}{c^2}, \qquad y_{26} = -x_1 A_{33} - x_6\xi_{33}^*,$$

$$y_{27} = \frac{(-x_1 A_{11} - x_6\xi_{11}^*)}{c^2} + \frac{(\zeta_{15} + \zeta_{31})}{c} - x_2 A_{33} - x_7\xi_{33}^*,$$

$$y_{28} = -\frac{(x_2 A_{11} + x_7\xi_{11}^*)}{c^2}, \qquad y_{29} = \zeta_{33} - x_3 A_{33} - x_8\xi_{33}^*,$$

$$y_{30} = \frac{(\zeta_{15} - x_3 A_{11} - x_8\xi_{11}^*)}{c^2}, \qquad y_{31} = \frac{e_3^*}{c} - \xi_{33}^* x_9 - A_{33}x_4,$$

$$y_{32} = -\frac{(x_4 A_{11} + x_9\xi_{11}^*)}{c^2}, \qquad y_{33} = -x_{10}\xi_{33}^* - x_5 A_{33} + e_3^*,$$

$$y_{34} = -\frac{(x_5 A_{11} + x_{10}\xi_{11}^*)}{c^2},$$

$$x_1 = -c_{44}dc,$$

$$x_2 = -\left(\frac{c_{11}}{c^2} - \overline{\rho}_{11}^{11}\right) dc - \frac{\left(m_{11}/c^2 - \overline{\rho}_{11}^{12}\right) c}{\widetilde{\zeta}_3} + \frac{\left(m_{11}/c^2 - \overline{\rho}_{11}^{12}\right)(e_{15} + e_{31})\, dc}{\widetilde{\zeta}_3},$$

$$x_3 = \frac{\left(m_{33}(e_{15} + e_{31})\, d - m_{33}\right)}{\widetilde{\zeta}_3} - (c_{13} + c_{44})\, d,$$

$$x_4 = -\left(\frac{m_{11}}{c^2} - \overline{\rho}_{11}^{12}\right) dc - \frac{\left(R/c^2 - \overline{\rho}_{11}^{22}\right) c}{\widetilde{\zeta}_3} + \frac{\left(R/c^2 - \overline{\rho}_{11}^{22}\right)(e_{15} + e_{31})\, dc}{\widetilde{\zeta}_3},$$

$$x_5 = \frac{\left(R(e_{15} + e_{31})\, d - R\right)}{\widetilde{\zeta}_3} - m_{11} d, \qquad x_6 = \frac{c_{44}\widetilde{\zeta}_3 dc}{e_3^*},$$

$$x_7 = \frac{\left(c_{11}/c^2 - \overline{\rho}_{11}^{11}\right) dc\widetilde{\zeta}_3}{e_3^*} - \frac{\left(m_{11}/c^2 - \overline{\rho}_{11}^{12}\right)(e_{15} + e_{31})\, dc}{e_3^*},$$

$$x_8 = \frac{(c_{13} + c_{44})\, d\widetilde{\zeta}_3}{e_3^*} - \frac{m_{33}(e_{15} + e_{31})\, d}{e_3^*},$$

$$x_9 = \frac{\left(m_{11}/c^2 - \overline{\rho}_{11}^{12}\right) dc\widetilde{\zeta}_3}{e_3^*} - \frac{\left(R/c^2 - \overline{\rho}_{11}^{22}\right)(e_{15} + e_{31})\, dc}{e_3^*},$$

$$x_{10} = \frac{m_{11} d\widetilde{\zeta}_3}{e_3^*} - \frac{R(e_{15} + e_{31})\, d}{e_3^*},$$

$$d = \frac{e_3^*}{\left(e_3^*(e_{15} + e_{31}) - \widetilde{\zeta}_3(\zeta_{15} + \zeta_{31})\right)},$$

$$d_{1i} = c_{55} p_i + \frac{(c_{55} r_{1i} + e_{15} r_{4i} + \zeta_{15} r_{5i})}{c},$$

$$d_{2i} = (c_{33} r_{1i} + m_{33} r_{3i} + e_{33} r_{4i} + \zeta_{33} r_{5i})\, p_i + \frac{(c_{31} + m_{33} r_{2i})}{c},$$

$$d_{3i} = \left(m_{33} r_{1i} + R r_{3i} + \widetilde{\zeta}_3 r_{4i} + e_3^* r_{5i}\right) p_i + \frac{(m_{11} + R r_{2i})}{c},$$

$$d_{4i} = \left(e_{33} r_{1i} + \widetilde{\zeta}_3 r_{3i} - \xi_{33} r_{4i} - a_{33} r_{5i}\right) p_i + \frac{\left(e_{31} + \widetilde{\zeta}_3 r_{2i}\right)}{c},$$

$$d_{5i} = (\zeta_{33} r_{1i} + e_3^* r_{3i} - a_{33} r_{4i} - \xi_{33}^* r_{5i})\, p_i + \frac{(\zeta_{31} + e_3^* r_{2i})}{c}. \tag{A.1}$$

References

[1] T. E. G. Alvarez-Arenas and F. M. De Espinosa, "Characterization of porous piezoelectric ceramics: the length expander case," *Journal of the Acoustical Society of America*, vol. 102, no. 6, pp. 3507–3515, 1997.

[2] T. E. G. Alvarez-Arenas, A. J. Mulholland, G. Hayward, and J. Gomatam, "Wave propagation in 0-3/3-3 connectivity composites with complex microstructure," *Ultrasonics*, vol. 38, no. 9, pp. 897–907, 2000.

[3] E. Roncari, C. Galassi, F. Craciun, C. Capiani, and A. Piancastelli, "A microstructural study of porous piezoelectric ceramics obtained by different methods," *Journal of the European Ceramic Society*, vol. 21, no. 3, pp. 409–417, 2001.

[4] C. R. Bowen, A. Perry, A. C. F. Lewis, and H. Kara, "Processing and properties of porous piezoelectric materials with high hydrostatic figures of merit," *Journal of the European Ceramic Society*, vol. 24, no. 2, pp. 541–545, 2004.

[5] B. P. Kumar, H. H. Kumar, and D. K. Kharat, "Study on pore-forming agents in processing of porous piezoceramics," *Journal of Materials Science*, vol. 16, no. 10, pp. 681–686, 2005.

[6] A. H. Nayfeh and H.-T. Chien, "The influence of piezoelectricity on free and reflected waves from fluid- loaded anisotropic plates," *Journal of the Acoustical Society of America*, vol. 91, no. 3, pp. 1250–1261, 1992.

[7] A. H. Nayfeh and H.-T. Chien, "Wave propagation interaction with free and fluid-loaded piezoelectric substrates," *Journal of the Acoustical Society of America*, vol. 91, no. 6, pp. 3126–3135, 1992.

[8] A. N. Darinskii and M. Weihnacht, "Acoustic waves guided by a fluid layer on a piezoelectric substrate," *Journal of Applied Physics*, vol. 104, no. 5, Article ID 054904, 9 pages, 2008.

[9] J. Liu and S. He, "Properties of Love waves in layered piezoelectric structures," *International Journal of Solids and Structures*, vol. 47, no. 2, pp. 169–174, 2010.

[10] A. K. Vashishth and V. Gupta, "Vibrations of porous piezoelectric ceramic plates," *Journal of Sound and Vibration*, vol. 325, no. 4-5, pp. 781–797, 2009.

[11] A. K. Vashishth and V. Gupta, "Wave propagation in transversely isotropic porous piezoelectric materials," *International Journal of Solids and Structures*, vol. 46, no. 20, pp. 3620–3632, 2009.

[12] A. K. Vashishth and V. Gupta, "Uniqueness theorem, theorem of reciprocity, and eigenvalue problems in linear theory of porous piezoelectricity," *Applied Mathematics and Mechanics*, vol. 32, no. 4, pp. 479–494, 2011.

[13] A. K. Vashishth and V. Gupta, "Reflection and transmission of plane waves from a fluid-porous piezoelectric solid interface," *Journal of the Acoustical Society of America*, vol. 129, no. 6, pp. 3690–3701, 2011.

[14] F. Levassort, J. Holc, E. Ringgaard, T. Bove, M. Kosec, and M. Lethiecq, "Fabrication, modelling and use of porous ceramics for ultrasonic transducer applications," *Journal of Electroceramics*, vol. 19, no. 1, pp. 125–137, 2007.

[15] P. Marechal, F. Levassort, J. Holc et al., "Electromechanical properties of piezoelectric integrated structures on porous substrates," *Ferroelectrics*, vol. 371, no. 1, pp. 89–97, 2008.

[16] R. Kar-Gupta and T. A. Venkatesh, "Electromechanical response of porous piezoelectric materials," *Acta Materialia*, vol. 54, no. 15, pp. 4063–4078, 2006.